DMD Fast Forward. Published on February 10, 2017 as DOI: 10.1124/dmd.116.074336
This article has not been copyedited and formatted. The final version may differ from this version.

Title Page

Novel Mechanism of Decyanation of GDC-0425 by Cytochrome P450

Ryan H Takahashi, Jason S Halladay, Michael Siu, Yuan Chen, Cornelis ECA Hop, S Cyrus Khojasteh, Shuguang Ma

Departments of Drug Metabolism and Pharmacokinetics (R.H.T, J.S.H.*, Y.C., C.E.H., S.C.K., S.M.) and Discovery Chemistry (M.S.), Genentech, Inc., 1 DNA Way, South San Francisco, CA, 94080

DMD Fast Forward. Published on February 10, 2017 as DOI: 10.1124/dmd.116.074336
This article has not been copyedited and formatted. The final version may differ from this version.

DMD # 74336

Running Title Page

Running Title: Trace circulating thiocyanate is derived from GDC-0425

Corresponding author: Ryan H. Takahashi, Drug Metabolism and Pharmacokinetics, Genentech, Inc., 1 DNA Way, MS 412a, South San Francisco, CA, 94080, Phone 650-225-1789, Email takahashi.ryan@gene.com

Text pages: 24

Table count: 2

Figure count: 7

Reference count: 22

Abstract: 246 words

Introduction: 523 words

Discussion: 1285 words

Abbreviations: ADME, absorption, distribution, metabolism, and excretion; AUC, area under the curve; ChK1, checkpoint kinase 1; CN^-, cyanide; CNS, central nervous system; LC-MS/MS, liquid chromatography-tandem mass spectrometry; $[M+H]^+$, protonated molecular ion; MS, mass spectrometry; P450, cytochrome P450; PK, pharmacokinetics; QD, quaque die (one a day); SCN^-, thiocyanate; TK, toxicokinetics.

DMD Fast Forward. Published on February 10, 2017 as DOI: 10.1124/dmd.116.074336
This article has not been copyedited and formatted. The final version may differ from this version.

Abstract

GDC-0425 is an orally bioavailable small molecule inhibitor of checkpoint kinase 1 (Chk1) that was investigated as a novel co-therapy to potentiate chemotherapeutic drugs such as gemcitabine. In the radiolabeled ADME study in Sprague-Dawley rats, trace level but long-lived ^{14}C-labeled plasma thiocyanate was observed. This thiocyanate originated from metabolic decyanation of GDC-0425 and rapid conversion of cyanide to thiocyanate. Excretion studies indicated decyanation was a minor metabolic pathway, but placing ^{14}C at nitrile magnified its observation. P450s catalyzed the oxidative decyanation reaction in vitro when tested with liver microsomes and, in the presence of $^{18}O_2$, one atom of ^{18}O was incorporated into the decyanated product. To translate this finding to a clinical risk assessment, the total circulating levels of thiocyanate (endogenous plus drug-derived) were measured following repeated administration of GDC-0425 to rats and cynomolgus monkeys. No overt increases were observed with thiocyanate concentrations of 121-154 µM in rats and 71-110 µM in monkeys receiving vehicle and all tested doses of GDC-0425. These findings were consistent with results from the radiolabel rat study where decyanation accounted for conversion of <1% of the administered GDC-0425 and contributed less than 1 µM thiocyanate to systemic levels. Further, in vitro studies showed only trace oxidative decyanation for humans. These data indicated that though cyanide was metabolically released from GDC-0425 and formed low levels of thiocyanate, this pathway was a minor route of metabolism and GDC-0425-related increases in systemic thiocyanate were unlikely to pose safety concern for subjects of clinical studies.

Introduction

GDC-0425 (5-((1-ethylpiperidin-4-yl)oxy)-9H-pyrrolo[2,3-b:5,4-c']dipyridine-6-carbonitrile, Figure 1) is a novel small molecule inhibitor of checkpoint kinase 1 (ChK1) that was discovered at Genentech, Inc. (South San Francisco, CA) (Gazzard et al., 2014). In nonclinical efficacy studies, administration of GDC-0425 in combination with chemotherapy agents resulted in abrogation of the S and G2/M checkpoint, premature entry into mitosis, and mitotic catastrophe, thus potentiating the anti-tumor effect of the chemotherapy agent. More specifically, Chik1 inhibitors, including GDC-0425, enhance the efficacy of gemcitabine in a broad range of preclinical models and in cancer cell lines that lacked p53 activity (Xiao et al., 2013). Thus, GDC-0425 was being developed for the treatment of patients with various advanced malignancies in combination with gemcitabine.

Preclinical data indicated that GDC-0425 had an adequate ADME profile to safely achieve clinical exposures for effective ChK1 inhibition with a daily oral dose regimen (unpublished data). Briefly, GDC-0425 was predicted to have low to moderate plasma clearance based on in vitro and preclinical animal PK data and low human plasma protein binding (60% unbound). The main metabolic pathways were characterized in vitro using human, rat, and monkey liver microsomes and included aromatic hydroxylation, *N*-dealkylation, and oxidation of the *N*-ethylpiperidine. Reaction phenotyping experiments using human liver microsomes with selective chemical inhibitors and individual recombinant P450s indicated that the drug metabolizing enzymes involved were CYP1A2, CYP2D6, and CYP3A. Data from the rat mass balance study using ^{14}C radiolabeled GDC-0425, described herein, indicated that drug-related radioactivity remained in circulation much longer than anticipated from the half-life of GDC-0425. Based on radioprofiling, this circulating analyte was later identified as thiocyanate.

Cyanide, which exists as prussic acid (HCN) when solubilized, is acutely toxic to humans (Ansell and Lewis, 1970; Hall and Rumack, 1986; Holland and Kozlowski, 1986). However, low level exposures to cyanide result in normal daily activity due to intake from the environment, cigarette smoke, and food sources. Evolutionarily, this necessitates highly efficient detoxification pathways for cyanide, which exist in humans and animals. The predominant pathway for cyanide deactivation is catalyzed by the mitochondrial enzyme rhodanase, which transfers sulfur from thiosulfate to cyanide to form thiocyanate, a less acutely toxic species (Ansell and Lewis, 1970). However, elevated levels of thiocyanate can also be a safety concern and have been implicated in the toxicities associated with long term infusions of nitroprusside in patients with severe renal dysfunction (Ansell and Lewis, 1970). Cyanide and thiocyanate exist at widely disparate concentration ranges in blood with cyanide reaching up to approximately 5 μM and thiocyanate reaching up to approximately 150 μM and both analytes can increase 2-3-fold upon cyanide exposures (Agency for Toxic Substances and Disease Registry, 2006).

Due to the potential risks associated with cyanide release and systemic thiocyanate, in vitro and in vivo studies were conducted to understand the decyanation of GDC-0425 decyanation prior to using GDC-0425 in a clinical trial. The pre-clinical studies suggested a low clinical risk, which has been verified by clinical data (Shin et al., 2015; Infante et al., 2016). This case study sets an example of prudent and measured risk assessment in response to an unexpected biotransformation, which could be critical for enabling the progression of clinical programs.

DMD Fast Forward. Published on February 10, 2017 as DOI: 10.1124/dmd.116.074336
This article has not been copyedited and formatted. The final version may differ from this version.

Materials and Methods

Materials. [^{14}C]GDC-0425 with the radiolabel located at the nitrile group was synthesized by Selcia Limited (Ongar, UK) with specific activity of 54.3 mCi/mmol and radiopurity of >99%. Potassium [^{14}C]cyanide was purchased from Moravek (Brea, CA) and ammonium thiocyanate was purchased from Sigma-Aldrich (St. Louis, MO). Oxygen-$^{18}O_2$ (99 atom %) was purchased from Sigma-Aldrich. All other chemicals used were obtained from commercial vendors at reagent quality or the highest quality available. Liver microsomes from rats pre-treated with corn oil (vehicle), β-naphthoflavone, or dexamethasone were purchased from Xenotech (Lenexa, KS) and from humans were purchased from BD Gentest (San Jose, CA).

Rat Mass Balance and PK

Animal study. The in-life and radioanalysis portions of the study were conducted by Covance (Madison, WI). Four groups of Sprague-Dawley rats from Hilltop Lab Animals, Inc. (Scottdale, PA) were administered a single oral dose of 10 mg/kg (200 μCi/kg) of [^{14}C]GDC-0425. The oral dose was prepared in 0.5% (w/v) methylcellulose, 0.2% (v/v) Tween 80 in deionized water. Group 1 was for mass balance (n=3 male and n=3 female); group 2 was for determination of biliary elimination (n=3 male and n=3 female, bile duct cannulated (BDC)), group 3 was for total radioactivity pharmacokinetics (PK) (n=3 male and n=3 female), and group 4 was for plasma collection for metabolite profiling (n=5 male and n=5 female). For Group 1 and 2 animals, urine, feces, and bile (group 2 only) were collected in plastic containers surrounded by dry ice predose (overnight for at least 12 h) and from 0-8 h, 8-24 h, and at 24-h intervals thereafter through 168 h (120 h for BDC animals) post-dose. For Group 3 animals, blood (approximately 0.35 mL) was collected from a jugular vein via syringe and needle, transferred into tubes containing K_2EDTA anticoagulant at 0.25, 0.5, 1, 3, 6, 12, 24, 48, 72, and 120 hours post-dose, and placed on wet ice

until aliquoted for radioanalysis and centrifuged to obtain plasma. For Group 4 animals, one animal/sex/time point was euthanized via exsanguination (cardiac puncture) under isoflurane anesthesia predose and at 1, 6, 12, 24, and 48 hours postdose and as much blood as possible was collected into tubes containing K_2EDTA anticoagulant. Samples were maintained on wet ice until centrifuged to obtain plasma.

Radioactivity Measurement. Blood and plasma were treated with a solubilizing agent and incubated for at least 1 h at approximately 60°C. Di-sodium EDTA (0.1 M) and hydrogen peroxide (30%) were added and samples were allowed to sit at least overnight to remove foaming and color. Ultima Gold XR scintillation cocktail was added and the samples were shaken and analyzed by liquid scintillation counting (LSC). Urine, bile, cage wash, and cage rinse were mixed with scintillation cocktail and duplicate weighed aliquots were analyzed by LSC. Fecal samples were homogenized with ethanol:water (1:1, v:v) and duplicate weighed aliquots were combusted with a Model 307 Sample Oxidizer (Packard Instrument Company) with the resulting $^{14}CO_2$ being trapped in a mixture of Perma Fluor and Carbo-Sorb and analyzed by LSC. LSC measurements were made for at least 5 minutes or 100,000 counts with a Model 2900TR (Packard Instrument Company).

Metabolite Profiling

Sample Preparation. Urine, bile, or feces were pooled for each gender with equal percentage of each collection. Plasma (1-2 g) and pooled fecal samples (1-2 g) were extracted with five volumes (volume or weight) of acetonitrile (ACN) with vortex mixing and sonicating, followed by centrifuging and removing the supernatants. The extraction was repeated one more time and supernatants were combined, evaporated to dryness, and reconstituted in a mix of the mobile

phases (ammonium acetate buffer, pH 5.0:ACN; 80:20 v:v) for radioprofile analysis. Reconstitution volumes were approximately 0.5 and 1.5 ml for plasma and feces extracts, respectively. Pooled urine and bile samples were vortex mixed and centrifuged to remove insoluble solids then analyzed.

LC-MS and Radioprofile Analysis. Liquid chromatography (LC) was performed using a 1200 Series system (Agilent Technologies, Santa Clara, CA) with a Luna C18(2) column (250×4.6 mm, 5 µm particle size, Phenomenex, Torrance, CA) that was heated constantly to 30^{o}C. The LC flow rate was 1.0 ml/min with mobile phases of 10 mM ammonium acetate, pH 5.0 (mobile phase A) and ACN (mobile phase B). A 57-min gradient elution was used with the following program: initial holding at 5% B for 5 min, then increasing to 30% B over 39 min, then increased to 95% B over 1 min and holding for 5 min to flush the column; and this was followed by re-equilibration at 5% B for 7 min before the next injection. The column effluent was split with approximately 25% diverted to the mass spectrometer and 75% to the radiometric detector or, for samples with less total radioactivity, a fraction collector for offline radiodetection. Online radioactivity measurements were made using a 610 TR radiodetector (Perkin Elmer) with a 0.5 mL flow cell and Ultima Flo M scintillation cocktail at a flow rate of 3 mL/min. Offline radioactivity measurements were made by collection of 10 second intervals per well into 96-well LumaPlate™-96 microplates (Perkin Elmer) and analysis by TopCount NXT™ scintillation and luminescence counter (Perkin Elmer).

A separate liquid chromatography method was developed to retain and confirm the identity of [^{14}C]thiocyanate in plasma samples. Chromatography was completed using an 1100 Series (Agilent Technologies) LC system with a Hypercarb column (100×4.6 mm, 5 µm particle size, Thermo Scientific) that was heated constantly to 30^{o}C. A gradient elution was used with mobile

phases of 0.005% diethylamine in water (mobile phase A) and 0.005% diethylamine in methanol (mobile phase B). The LC flow rate was 1.0 mL/min. Analytes were eluted from the column with the following gradient: initial holding at 0% B for 5 min, then increased to 50% B over 15 min, then increased to 95% B over the following 5 min and held for 5 min to flush the column. The column was re-equilibrated for 5 min at 5% B before the next injection.

A LTQ Orbitrap XL high resolution mass spectrometer (Thermo Scientific, San Jose, CA) was used to obtain full scan and product ion spectra for metabolite identification. Column eluent was introduced with an electrospray ionization source with voltage set at 5 kV and heated capillary at 275°C. The capillary and tube lens voltages were set at 40 and 95 V, respectively. The full scan event cycle was used as a survey scan upon which MS/MS scans were completed following collision induced dissociation and higher energy collision dissociation.

In Vitro Incubations to Identify Decyanation Products. Metabolic reactions contained microsomal protein (0.5 mg/ml) in potassium phosphate, pH 7.4 (100 mM) supplemented with magnesium chloride (3 mM) and NADPH (1 mM). Reactions were initiated by adding GDC-0425 (5 µM). For metabolite-searching experiments, an equimolar mix of natural and deuterated (d_9-piperidine) GDC-0425 was incubated so that the isotope ratio would confirm that an analyte originated from the test compound. At the end of the incubation (60 min), the reactions were quenched with three volumes of cold ACN, and proteins were precipitated. The supernatants were concentrated under vacuum for analysis.

Similar incubations were conducted with liver microsomes and either d_0-GDC-0425 or d_9-GDC-0425 as substrate under an atmosphere of $^{18}O_2$. Similar experimental setups have been previously reported by other investigators to confirm the contribution of P450s (Zhang et al., 2002). The

reaction mixture components except microsomes were placed in the reaction vessel and air was evacuated from the headspace and solution by three successive rounds of freezing in a dry ice-acetone bath, pumping under vacuum for several minutes, and thawing at ambient temperature. $^{18}O_2$ was introduced to the vessel, and then reactions were started by adding microsomes via syringe injection and kept at 37°C for one hour. The reactions were quenched with an equal volume of cold ACN and analyzed.

Repeated Dose TK Studies in Rats and Monkeys

In-Life Study. The oral tolerability (toxicity) and toxicokinetics (TK) of GDC-0425 were evaluated following oral gavage administration in male and female Sprague-Dawley rats and cynomolgus monkeys over four weeks. Rats received either vehicle or GDC-0425 at 6, 20, or 60 mg/kg on three consecutive days each week. Separate animals (3 per sex per group) were assigned for TK analysis. Male and female naïve monkeys (Covance Research Products, Alice TX and Denver, PA) received either control vehicle or GDC-0425 at dose levels of 2, 6, or 20 mg/kg. For rats and monkeys, GDC-0425 was administered in a vehicle of 0.5% (w/v) methylcellulose and 0.2% (w/v) polysorbate 80 (Tween 80) in reverse osmosis water and the dose volumes were 5 ml per kg animal body weight. For TK analysis, blood samples (approximately 0.5 mL) were collected via a jugular vein from three animals per group per sex predose and at 1, 4, 8, 12, and 24 h post-dose on Study Days 1 and 24. Blood samples were placed into tubes containing K_2EDTA and maintained chilled until plasma samples were harvested and stored at −80°C until analysis.

Measurement of GDC-0425 in Plasma. Rat and monkey TK plasma were assayed for GDC-0425 concentrations using validated bioanalytical assays. Details of the assay are similar to those

that were subsequently validated for determining GDC-0425 concentrations in clinical plasma samples (Ding et al., 2016). Chromatography was completed on an Aquasil C18, 50x2.1 mm, 5 µm column (Thermo Scientific, San Jose, CA) with gradient elution of mobile phases composed of 0.1% formic acid in water:100 mM formate (9:1, v:v) and 0.1% formic acid in ACN:100 mM ammonium formate (9:1, v:v) with a flow rate of 1.2 ml/min. GDC-0425 and d_9-GDC-0425 (internal standard) were monitored using positive ion electrospray with the MRM transitions *m/z* 322.3→98.1 and *m/z* 331.3→107.3, respectively. The quantitative range for GDC-0425 concentrations was 0.003 to 1.6 µM.

Measurement of Thiocyanate in Plasma. The concentrations of thiocyanate in rat and monkey TK plasma samples were measured using a colorimetric ferric-cyanate complex. This method was subsequently validated for the measurement of plasma levels of thiocyanate in a Phase I clinical study in cancer patients treated with GDC-0425 and have been reported (Shin et al., 2015). Due to endogenous thiocyanate in plasma, calibration standards and quality control samples were prepared in phosphate-albumin buffered saline (pH 7.2). The quantitative range of the method was 25 to 500 µM.

Results

Mass Balance, Excretion Profiles, and Pharmacokinetics of Radioactivity. No differences were observed between male and female rats in the rates or extent of recoveries for radioactivity; therefore, data were grouped and are described with the average of all animals. After a single oral administration of [^{14}C]GDC-0425 to Sprague-Dawley rats, 96.4% of the administered radioactivity was recovered. Elimination was rapid with 94% of the dose recovered in the first 48

h post-dose. The majority of the radioactivity (60.4% of the dose) was recovered in feces and the remaining (34.1%) was recovered in urine. For BDC rats, 31.2% of the administered radioactivity was recovered in bile and 47.9% was recovered in urine. This indicated that the oral dose of GDC-0425 had been well absorbed (i.e., at least 79.1% of the dosed radioactivity had been absorbed) (Supplemental Figure 1).

Total radioactivity plasma exposures ($AUC_{0\text{-}48h}$) were 112 µM*h, reaching maximal concentrations of 7.0 µM at approximately 1 h post-dose and declining to 0.32 µM at 120 h post-dose with a half-life of 63 h. The blood to plasma ratios were 0.7-0.9 for the first 12 h post-dose and approximately 1.0 at later time points. There were no clear PK differences (AUC or C_{max}) between male and female rats.

Metabolite Profiling of Rat Samples. Representative plasma radioprofiles are shown in Figure 2. Proposals for chemical structures for metabolites were based on chemical formulas derived from accurate mass measurements of protonated molecular ions and the interpretation of the product ions. The summarized data for structural elucidation of metabolites are described in Table 1 and the metabolic pathways for GDC-0425 observed in rats are summarized in Figure 3.

To confirm the identity of the early-eluting radioactivity, a second chromatographic method was employed that retained highly-polar analytes and provided MS confirmatory information. Analysis of authentic standards for thiocyanate and cyanide demonstrated that this method was successful at chromatographically retaining and resolving these analytes (elution at 6 and 11 min, respectively) and enabled identifying them based on their MS molecular ions. The early-eluting radioactivity in plasma was confirmed to be thiocyanate with its retention time matching the

standard and a molecular ion observed in negative ion mode at *m/z* 57.9769 (Δ=0.012 Da (20.7 ppm)). Cyanide was not detected in these samples.

Plasma concentrations for GDC-0425 and its metabolites are shown in a concentration-time plot (Figure 4) and calculated as percentage of total radioactivity exposures in Table 2. GDC-0425 reached its maximal plasma concentrations of 6.5 µM at 1 h post-dose with a terminal half-life of 3.6 h. Its exposure accounted for 36.1% of plasma radioactivity ($AUC_{0\text{-}48\ h}$). The radioprofiles of plasma at later time points indicated the major circulating species was thiocyanate (Figure 2). Thiocyanate accounted for 37.0% of plasma radioactivity ($AUC_{0\text{-}48\ h}$), was observed at its maximal concentration of 0.73 µM at 12 h post-dose and then declined at the same rate as total radioactivity. The other abundant circulating metabolites were present at lower levels and included M10 (*N*-deethyl) and M16 (ketone metabolite), which accounted for 3.2 and 9.0% of plasma radioactivity ($AUC_{0\text{-}48h}$), respectively.

The profiles of GDC-0425 and its metabolites in urine, feces, and bile are summarized in Table 2. GDC-0425 in bile was negligible, but in urine accounted for 11% of the dose, indicating the contribution of renal clearance. Unchanged GDC-0425 in feces accounted for only 5.3% of the dose, which indicated that the oral dose had been well-absorbed and that the majority of clearance was by metabolism. The major metabolites in urine were M10 (*N*-deethylation) and M5 (*O*-dealkylation), which accounted for 9.7% and 3.6% of the dose, respectively. In bile, the M6 (hydroxylation and glucuronidation) and M9 (hydroxylation) were observed and accounted for 10.6 and 5.3% of the dose, respectively. In feces, the major metabolites were M7 (*N*-dealkylation and hydroxylation), M9 (hydroxylation), and M10 (*N*-deethylation), which accounted for 5.0%, 22.9%, and 11.6.3% of the dose, respectively. The remaining radioactivity

DMD Fast Forward. Published on February 10, 2017 as DOI: 10.1124/dmd.116.074336
This article has not been copyedited and formatted. The final version may differ from this version.

in these samples was split over minor metabolites that individually accounted for ~2% or less of the dose.

Identification of GDC-0425 Decyanation Products. An oxidative product, M18, was identified during in vitro experiments, where it was observed as a low level metabolite in rat and human liver microsome incubations, but was notably more abundant in dexamethasone-pretreated rat liver microsome incubations. The $[M+H]^+$ for M18 was observed at *m/z* 313.1657 ($C_{17}H_{21}N_4O_2^+$, -0.51 ppm). The base peak in the MS/MS spectrum was observed at *m/z* 112, which corresponded to unchanged *N*-ethylpiperidine, and other identifying product ions were observed at *m/z* 202 and 268, which were generated via cleavages of the piperidine ring (Figure 5). These ions were consistent with replacement of the nitrile of GDC-0425 with a hydroxyl.

^{18}O-Labeling experiments were conducted in which d_0-GDC-0425 and d_9-GDC-0425 were separately incubated with rat liver microsomes in the presence of $^{18}O_2$. Incorporation of ^{18}O was determined by LC-MS/MS analysis and was based on the observed relative intensities of $[M+H]^+$ ions for M18 and M9 at the following *m/z* (Δ5 ppm): d_0-M18, ^{16}O=313.1659, ^{18}O=315.1702; d_9-M18, ^{16}O=322.2223, ^{18}O=324.2266; d_0-M9, ^{16}O=338.1612, ^{18}O=340.1654; d_9-M9, ^{16}O=347.2176, ^{18}O=349.2218. The products formed under the atmosphere of $^{18}O_2$ incorporated one atom of ^{18}O at 94-98% excess. The MS/MS spectra following CID of the $[M+H]^+$ ions for unlabeled d_0-M18, ^{18}O-labeled d_0-M18, and ^{18}O-labeled d_9-M18 are shown in Figure 5. The ions at *m/z* 202 and 268 in unlabeled d_0-M18 were shifted 2 Da higher in the ^{18}O-labeled metabolite, consistent with the incorporation of the ^{18}O at the aromatic hydroxyl moiety. The corresponding metabolite formed from d_9-GDC-0425 in presence of $^{18}O_2$ showed a product ion at *m/z* 205 resulting from incorporation of one ^{18}O atom and transfer of one deuterium from piperidine on dissociation. Because the incubations were conducted without radiolabeled substrate and

presumed low or absent activities for rhodonase in vitro, cyanide and thiocyanate were not monitored.

The primary decyanation product of GDC-0425, M18, was not detected in the rat in vivo samples. Instead, a metabolite presumed to arise from further metabolism of M18 was identified. This metabolite, identified as M17, was a glucuronide conjugate of hydroxylated M18, which was detected by mass spectrometry in urine and bile samples with its protonated molecular ion at *m/z* 505.1928 ($C_{23}H_{29}N_4O_9^+$, -0.2 ppm). Upon MS/MS of this ion, a neutral loss of 176 Da (glucuronic acid) provided the aglycone at *m/z* 329 and in MS^3 experiments, an ion at *m/z* 112 was observed, which indicated the *N*-ethylpiperidine was unchanged. As expected for the decyanation products of [^{14}C]GDC-0425, there was no corresponding peak observed in the radioprofile.

Repeated Dose Rat and Monkey TK Studies

GDC-0425 and Thiocyanate in Rat. The mean plasma concentration-time profiles are presented in Figures 6A and 6B and full data are provided as Supplemental Table 1. No sex differences in PK were apparent, so male and female animals are described as a single group. Exposures for GDC-0425 generally increased with dose from 6 to 60 mg/kg and following multiple doses. Increases in C_{max} were generally less than dose proportional while the increases in AUC_{0-24} were roughly dose proportional. Exposures on Day 24 were approximately 2 to 3-fold higher than on Day 1. No apparent differences between control and treatment groups in plasma thiocyanate were observed with measured concentrations (mean and 95% confidence intervals) of 150 (145-154), 143 (139-148), 131 (125-137), and 127 (121-134) µM in rats receiving vehicle (control), 6, 20, and 60 mg/kg of GDC-0425, respectively. The thiocyanate exposures,

determined as $AUC_{0\text{-}24h}$, were not different between the first dose (Day 1) and repeated dose (Day 24) for any of the dose groups.

GDC-0425 and Thiocyanate in Monkey. The mean plasma concentration-time profiles are presented in Figures 6C and 6D and full data are provided as Supplemental Table 1. There were no apparent sex differences in PK profile (C_{max} or $AUC_{0\text{-}24}$), so male and female animals are described as a single group. GDC-0425 exposures increased with increasing dose though were less than dose proportional. In general, exposures were higher following multiple doses with slightly higher (less than 2-fold) mean C_{max} and $AUC_{0\text{-}24}$. GDC-0425 was readily absorbed after oral gavage administration and maximal plasma concentrations were observed at 1 or 4 h post-dose on Days 1 and 24. No differences in plasma thiocyanate were observed between control and treatment groups with measured concentrations (mean and 95% confidence intervals) of 93 (85-102), 98 (85-110), 88 (77-98), and 78 (71-86) µM in monkeys that received vehicle (control), 2, 6, and 20 mg/kg of GDC-0425, respectively. As observed with rats, thiocyanate exposures did not differ between the first dose and repeated dose for any of the dose groups.

Discussion

To support the clinical development of GDC-0425, a radiolabeled rat mass balance and metabolite identification study was conducted. The ease of addition of [^{14}C]nitrile group in the final synthetic step was one reason for the placement of the radiolabel. The risk of losing the radiolabel was assessed in vitro, which indicated that it was stable. Following a single oral administration at 10 mg/kg (200 µCi/kg), the radioactive dose was rapidly and well absorbed. Clearance was mainly through oxidative metabolism (65% of the administered dose) and renal

excretion (11% of the administered dose) with minor contribution by biliary secretion (less than 1%). The observed metabolic pathways were consistent with in vitro experiments with the predominant pathways being P450-mediated oxidation (*N*-deethylation, *O*-dealkylation, and hydroxylation) followed by UGT-mediated conjugation.

The long apparent half-life for plasma radioactivity (63 h) was not anticipated based on in vitro or in vivo PK (non-radiolabeled) studies. Radioprofiling of the plasma samples confirmed this to be attributed to an unexpected polar metabolite (M1) in plasma that retained the radiotracer. Subsequent experiments using a Hypercarb column allowed this analyte to be chromatographically retained and showed it to be a single chromatographic peak that was identified as thiocyanate. This analysis also provided selective quantification of the drug-derived thiocyanate, which reached a maximal plasma concentration of approximately 0.7 μM followed by a slow decline that explained the long-lived circulating radioactivity (Figure 4). Radioprofiling of excreta samples showed that thiocyanate was eliminated in urine, bile, and feces (≤0.3% of the dose per elimination route). It was evident based on retention of the radiolabel that thiocyanate had originated from GDC-0425, which indicated that GDC-0425 had undergone a decyanation reaction and the released cyanide had been efficiently converted to thiocyanate. The latter was well-supported by the known high activities for rhodonase. The decyanation reaction accounted for less than 1% of the GDC-0425 dose; however, it was a pronounced observation due to the low volume of distribution and slow clearance of thiocyanate and the placement of ^{14}C at the nitrile group.

Metabolic cyanide release is a relatively uncommon reaction (Fleming et al., 2010) and few previous examples have been reported. For a thrombin inhibitor, a pyrazinone ring was rationalized to be bioactivated by forming an epoxide intermediate, which upon ring-opening

released cyanide (Lin et al., 2005). For tofacitinib (a janus kinase inhibitor), mechanistic studies demonstrated that CYP3A4-mediated oxidation occurred at the α-carbon to the nitrile group, which upon dissociation to the corresponding aldehyde eliminated cyanide (Le et al., 2016). In the case of the natural cofactor vitamin B12 (cyanocobalamin), cyanide was released via reductive elimination catalyzed by cytosolic oxidoreductase enzymes (Kim et al., 2008). Finally, in the cases of verapamil and amygdalin, anaerobic bacteria, which may exist in the intestinal flora, are suggested to catalyze elimination of primary or secondary nitrile groups (Newmark et al., 1981; Koch and Palicharla, 1990). Though there was precedence for cyanide being metabolically released from a drug, these proposed mechanisms did not satisfactorily describe how it had occurred from GDC-0425. In this case, the nitrile group was attached to an aromatic ring system, which would presumably be less susceptible for carbon-carbon cleavage.

A decyanation product, M18, was observed in the rat and human liver microsomes incubation samples. Based on mass spectrometric data, the nitrile of GDC-0425 was replaced with hydroxyl group. The formation of this metabolite was NADPH-dependent and more extensive in liver microsomes from dexamethasone pre-treated rats compared to those from vehicle pre-treated rats, which were suggestive that P450s were involved. The role for P450s in the oxidative decyanation reaction was tested and confirmed in ^{18}O labeling experiments. Both M18 and M9, the aromatic hydroxylation product, formed with incorporation of one ^{18}O atom when GDC-0425 was incubated with liver microsomes in the presence of $^{18}O_2$. M18 was not found in the rat in vivo samples; however, metabolite scouting showed M18 may have undergone further metabolism (oxidation and glucuronidation) to M17 prior to being eliminated. M17 was observed as a low-level metabolite in urine and bile samples based on MS detection.

Based on M18 as the putative primary product of the P450-mediated decyanation reaction, we propose the mechanism shown in Figure 7. We describe nucleophilic addition of the P450 peroxo-anion intermediate species to carbon-2 of pyridine (step 1). This reaction center could be rationalized to be determined by the electron-withdrawing nitrogen and nitrile moiety. In a concerted rearrangement of this tetrahedral transition state, the O-O bond is cleaved and cyanide anion is released (step 2). This product can then tautomerize to its pyridine-2-ol form, M18 (step 3). We have considered formation of an electrophilic intermediate, such as epoxide, at pyridine, then oxygen addition which displaces the nitrile; however, in vitro trapping studies using the thiol-containing reagents glutathione and cysteine provided no evidence of this intermediate. Further, though we describe the oxidation reaction as a two-electron addition to the aromatic ring, it is possible that this reaction could occur via a single electron abstraction forming a delocalized radical cation that binds an activated oxygen species of P450. Several sources have described these reactions and the observations supporting these possible mechanisms (Vaz, 2003; Ortiz de Montellano and De Voss, 2005; Testa and Kramer, 2008).

Though decyanation had occurred as a minor metabolic pathway in rats, it was judged prudent to assess its extent in repeated dose studies of GDC-0425 in rats and monkeys. In these studies, total plasma (endogenous plus GDC-0425-derived) thiocyanate concentrations were monitored and demonstrated there were no differences between animals receiving vehicle or any tested dose of GDC-0425. Further, there were no observed effects on respiration rates or oxygen saturation levels and no CNS findings that would be indicative of cyanide or thiocyanate toxicity. These data confirmed the findings from the in vitro and radiolabeled rat studies and further supported that GDC-0425-derived thiocyanate was negligible. The corresponding in vitro human data were indicative that decyanation reaction would be minor in humans. To make a

conservative assessment of clinical risk, a scenario of an extreme case of decyanation was considered. If 2% of administered GDC-0425 underwent decyanation (magnitudes greater than predicted based on in vitro and preclinical evidence), the starting clinical dose of 60 mg QD could result in an addition of approximately 1 μM thiocyanate to systemic levels. This would contribute negligibly to endogenous thiocyanate, which exists at significantly higher and highly variable concentrations of 34 μM in serum and up to 100 μM in smokers (Foss and Lund-Larsen, 1986).

In the phase 1 first-in-human clinical trial, GDC-0425 was orally administered daily at 60 mg or 80 mg in combination with a standard dose of gemcitabine to cancer patients (Infante et al., 2016). Measurements of total plasma thiocyanate were included in the patient monitoring, which demonstrated that thiocyanate levels were unchanged following GDC-0425 administration and remained below 150 μM for all subjects (Shin et al., 2015). These results confirmed the negligible contribution to systemic thiocyanate by decyanation of GDC-0425 in humans and demonstrated the conservative nature of the clinical risk assessment that assumed 2% of the dose undergoing conversion to thiocyanate. These findings were part of the clinical safety profile of GDC-0425 established in the phase I study.

In conclusion, P450 enzymes catalyzed the release of cyanide from GDC-0425, which was subsequently converted to systemic thiocyanate in vivo. A radiolabeled study of GDC-0425 demonstrated that this metabolic pathway was a minor route of clearance. Thiocyanate levels were determined in multiple-dose toxicological studies of GDC-0425 in rats and monkeys and indicated that there were no increases in systemic thiocyanate concentrations arising from GDC-0425 administration. These pre-clinical studies supported that thiocyanate formation was

unlikely to be a safety concern for patients receiving GDC-0425, which was confirmed by negligible changes in thiocyanate exposures in the phase I study.

Acknowledgements

We thank Drs Shana Dalton, Michael Fitzsimmons, David Peters, and Madhu Sanga, and the research staff at Covance Inc for conducting the preclinical studies; Henri Meijering and colleagues at QPS Netherlands B.V. for determining thiocyanate concentrations; and our colleagues at Genentech, Inc.: Drs Xiao Ding, Young Shin, Jennifer Schutzman, and all members of the Chk1 project team.

Author Contributions

Participated in research design: Takahashi, Halladay, Hop, Khojasteh, Ma

Conducted experiments: Takahashi, Halladay, Siu

Contributed new reagents or analytic tools: Siu

Performed data interpretation: Takahashi, Halladay, Khojasteh, Ma

Contributed to the writing of the manuscript: Takahashi, Chen, Khojasteh, Ma

References

Ansell M and Lewis FA (1970) A review of cyanide concentrations found in human organs. A survey of literature concerning cyanide metabolism, 'normal', non-fatal, and fatal body cyanide levels. J Forensic Med 17:148-155.

Ding X, Chen Y, Sahasranaman S, Shi Y, McKnight J, and Dean B (2016) A supported liquid extraction LC-MS/MS method for determination of concentrations of GDC-0425, a small molecule Checkpoint kinase 1 inhibitor, in human plasma. Biomed Chromatogr 30:1984-1991.

Fleming FF, Yao L, Ravikumar PC, Funk L, and Shook BC (2010) Nitrile-containing pharmaceuticals: efficacious roles of the nitrile pharmacophore. J Med Chem 53:7902-7917.

Foss OP and Lund-Larsen PG (1986) Serum thiocyanate and smoking: interpretation of serum thiocyanate levels observed in a large health study. Scand J Clin Lab Invest 46:245-251.

Gazzard L, Appleton B, Chapman K, Chen H, Clark K, Drobnick J, Goodacre S, Halladay J, Lyssikatos J, Schmidt S, Sideris S, Wiesmann C, Williams K, Wu P, Yen I, and Malek S (2014) Discovery of the 1,7-diazacarbazole class of inhibitors of checkpoint kinase 1. Bioorg Med Chem Lett 24:5704-5709.

Hall AH and Rumack BH (1986) Clinical toxicology of cyanide. Ann Emerg Med 15:1067-1074.

Holland MA and Kozlowski LM (1986) Clinical features and management of cyanide poisoning. Clin Pharm 5:737-741.

Infante JR, Hollebecque A, Postel-Vinay S, Bauer TM, Blackwood E, Evangelista M, Mahrus S, Peale F, Lu X, Sahasranaman S, Zhu R, Chen Y, Ding X, Murray E, Schutzman J,

Lauchle JO, Soria JC, and LoRusso PM (2016) Phase I Study of GDC-0425, a checkpoint kinase 1 inhibitor, in combination with gemcitabine in patients with refractory solid tumors. Clin Cancer Res doi: 10.1158/1078-0432.CCR-16-1782. Published Online First November 4, 2016.

Kim J, Gherasim C, and Banerjee R (2008) Decyanation of vitamin B12 by a trafficking chaperone. Proc Natl Acad Sci U S A 105:14551-14554.

Koch RL and Palicharla P (1990) The anaerobic metabolism of verapamil in rat cecal contents forms nor-verapamil and thiocyanate. J Pharmacol Exp Ther 254:612-615.

Le H, Fan PW, Wong S, Ma S, Driscoll JP, Hop CE, and Cyrus Khojasteh S (2016) Elucidating the Mechanism of Tofacitinib Oxidative Decyanation. Drug Metab Lett 10:136-143.

Lin CC, Wong BK, Burgey CS, Gibson CR, and Singh R (2005) In vitro metabolism of a thrombin inhibitor and quantitation of metabolically generated cyanide. J Pharm Biomed Anal 39:1014-1020.

Newmark J, Brady RO, Grimley PM, Gal AE, Waller SG, and Thistlethwaite JR (1981) Amygdalin (Laetrile) and prunasin beta-glucosidases: distribution in germ-free rat and in human tumor tissue. Proc Natl Acad Sci U S A 78:6513-6516.

Ortiz de Montellano PR and De Voss JJ (2005) Substrate Oxidation by Cytochrome P450 Enzymes, in: Cytochrome P450: structure, mechanism, and biochemistry (Ortiz de Montellano PR ed), pp 183-230, Kluwer Academic/Plenum Publishers, New York.

Shin YG, Meijering H, van Heuveln FH, Wieling J, Halladay J, Sahasranaman S, and Hop CECA (2015) Validation of a method for the determination of thiocyanate in human plasma

by UV/VIS spectrophotometry and application to a Phase I clinical trial of GDC-0425. Transl Clin Pharmacol 23:59-65.

Testa B and Kramer SD (2008) The Biochemistry of Drug Metabolism: Principles, Redox Reactions, Hydolyses. Verlag Helvetica Chimica Acta, Zurich, Switzerland.

Vaz ADN (2003) Dioxygen activation by chtochromes P450: A role for multiple oxidants in the oxidation of substrates, in: Drug Metabolizing Enzymes: Cytochrome P450 and Other Enzymes in Drug Discovery and Development (Lee JS, Obach RS, and Fisher MB eds), pp 1-27, Marcel Dekker Inc., New York, NY.

Xiao Y, Ramiscal J, Kowanetz K, Del Nagro C, Malek S, Evangelista M, Blackwood E, Jackson PK, and O'Brien T (2013) Identification of preferred chemotherapeutics for combining with a CHK1 inhibitor. Mol Cancer Ther 12:2285-2295.

Zhang Z, Li Y, Stearns RA, Ortiz De Montellano PR, Baillie TA, and Tang W (2002) Cytochrome P450 3A4-mediated oxidative conversion of a cyano to an amide group in the metabolism of pinacidil. Biochemistry 41:2712-2718.

Footnotes

Current Affiliation for J.S.H.: Department of Drug Metabolism and Pharmacokinetics, Anacor Pharmaceuticals, Inc., Palo Alto, CA

Legends for Figures

Figure 1. Chemical structure of GDC-0425 which indicates the location of the ^{14}C radiolabel at the nitrile moiety.

Figure 2. Representative radioprofiles for plasma from rats administered a single 10 mg/kg (200 µCi/kg) oral dose of [^{14}C]GDC-0425. Radioprofiles to measure metabolite abundances were conducted following chromatography on a Luna C18(2) (250×4.6 mm, 5 µm) column, which did not retain cyanide and thiocyanate and these analytes eluted at the column dead volume (ca. 3.5 min).

Figure 3. Proposed metabolic pathways for GDC-0425 in rats. For clarity, only major pathways (i.e., metabolite accounted for >10% of the dose in excreta or >10% of the plasma exposures to drug-related material) and the oxidative decyanation pathways are shown. The rat samples containing the metabolite are described with P=plasma, U=urine, F=feces, and B=bile.

Figure 4. Plasma concentration-time profiles for total radioactivity, unchanged GDC-0425, and abundant circulating metabolites measured for rats following a single oral administration of 10 mg/kg (200 µCi/kg) [^{14}C]GDC-0425. Data are presented as mean and standard deviation for total

radioactivity (n=6, 3 male and 3 female rats) and single measurements for other analytes (composite PK curve).

Figure 5. Product ion spectra obtained for the oxidative decyanation metabolite, M18, and proposed fragmentation following collision induced dissociation. Spectra are shown for M18 formed in liver microsomes incubation of (A) d_0-GDC-0425, (B) d_0-GDC-0425 in $^{18}O_2$ atmosphere, and (C) d_9-GDC-0425 in $^{18}O_2$ atmosphere. Proposed product ions are shown with theoretical masses.

Figure 6. Plasma concentration-time profiles for GDC-0425 (left) and thiocyanate (right) measured on Days 1 and 24 in repeated daily oral dose studies of GDC-0425 administered to (A and B) rats at 6, 20, and 60 mg/kg and (C and D) monkeys at 2, 6, and 20 mg/kg. Data are presented as mean and standard deviation (n=6, 3 male and 3 female animals each).

Figure 7. Proposed mechanism for oxidative decyanation of GDC-0425 catalyzed by P450.

Table 1. Mass spectrometric data for GDC-0425 and its metabolites with proposed structural elucidation.

Analyte	Observed MH^+ (Chemical Formula, Mass accuracy in parts per million)	Characteristic Product Ions (*m/z*)	Structure and MS/MS Product Ions
GDC-0425	322.1665 ($C_{18}H_{20}N_5O^+$, 0.9)	112 (100), 98, 84, 70, 58	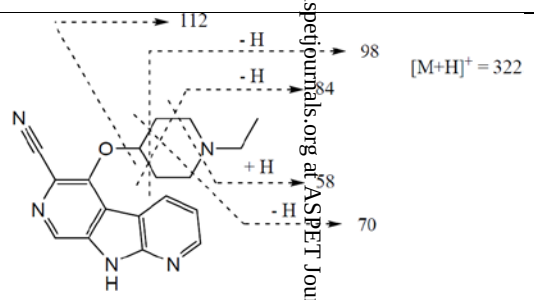
M1	57.9769 (negative ion) (SCN^-, 21)	N/A	Thiocyanate
M5	211.0614 ($C_{11}H_7N_4O^+$, 0)	193, 184 (100), 156	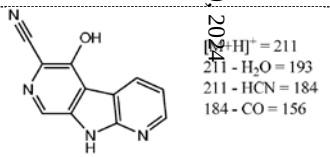
M7	310.1299 ($C_{16}H_{16}N_5O_2^+$, 0)	293, 227 (100), 84, 56	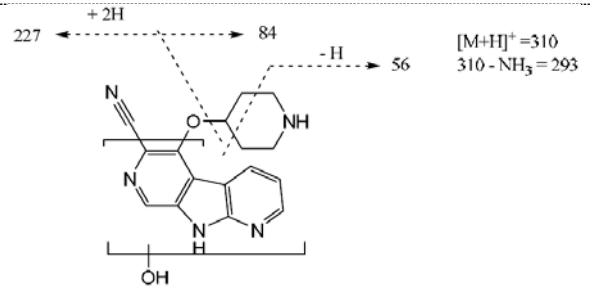

M9	338.1611 ($C_{18}H_{20}N_5O_2^+$, -0.3)	320, 254, 227, 112 (100), 98, 84, 70, 58	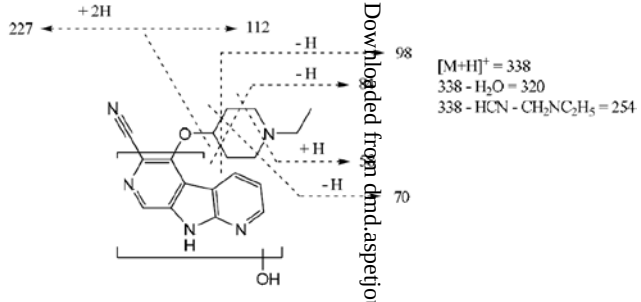
M10	294.1348 ($C_{16}H_{16}N_5O^{+,}$ -0.3)	211, 84 (100), 56	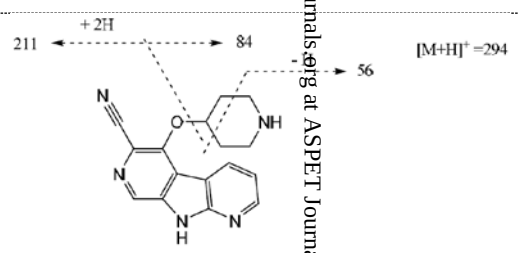
M14	338.1611 ($C_{18}H_{20}N_5O_2^+$, -0.3)	320, 306 (100), 278, 251, 128, 112, 110, 74	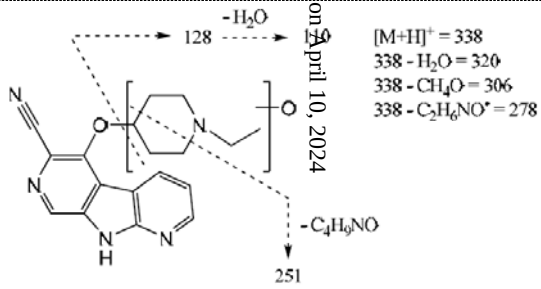
M16	336.1454 ($C_{18}H_{18}N_5O_2^+$, -0.3)	294, 253, 211 (100), 126, 84, 56	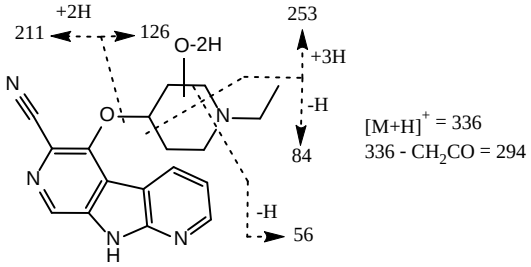

M17	505.1928 ($C_{23}H_{29}N_4O_9^+$, -0.2)	329 (100), 254, 112, 98, 84	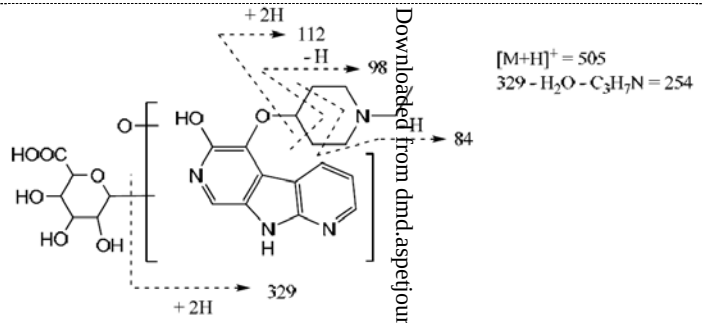
M18	313.1657 ($C_{17}H_{21}N_4O_2^+$, -0.5)	268, 202, 112 (100)	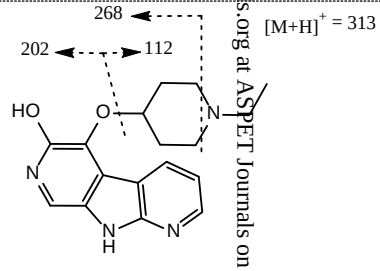

Glucuronide conjugates were observed with $[M+H]^+$ at 176 Da mass shift higher than their corresponding aglycones. Other than M17, for which the corresponding aglycone was not detected, the conjugates have not been listed but were assigned unique metabolite identifiers.

DMD Fast Forward. Published on February 10, 2017 as DOI: 10.1124/dmd.116.074336
This article has not been copyedited and formatted. The final version may differ from this version.

Table 2. GDC-0425 and its metabolite measured in plasma and excreta following a single oral administration to Sprague-Dawley rats

Analyte	Biotransformation	Plasma	% of Dose Recovered		
		% of TRA 0-48 h	Urine	Feces	Bile*
GDC-0425	Parent compound	36.1	11.0	5.29	0.64
M1	Thiocyanate	37.0	0.06	0.31	0.08
M2	Glucuronidation	ND	1.31	0.87	2.11
M3	*O*-Dealkylation+ Glucuronidation	ND	1.31	ND	D
M4	*N*-Deethylation+ Hydroxylation+Glucuronidation	ND	ND	ND	2.33
M5	*O*-Dealkylation	D	3.61	2.34	0.49
M6	Hydroxylation+Glucuronidation	D	0.53	ND	10.6
M7	*N*-Deethylation+Hydroxylation	ND	0.41	5.00	1.29
M9	Hydroxylation	D	1.81	22.9	5.28
M10	*N*-Deethylation	3.17	9.74	11.6	1.82
M14	Hydroxylation	D	1.71	D	1.82
M16	Oxidation (+14 Da)	9.00	0.78	2.64	0.14
	% Dose	N/A	32.7	59.1	30.9*

ND, not detected; D, detected by mass spectrometry; TRA, total radioactivity.

* Bile were collected from surgicalized animals that were separate from the animals which are described for urine and feces.

Plasma are mean results for male and female rats (n=1 per sex per time point). Urine and feces are mean results for bile-duct intact animals (n=3 per sex) and bile are mean results for bile-duct cannulated animals (n=3 per sex).

Figure 1

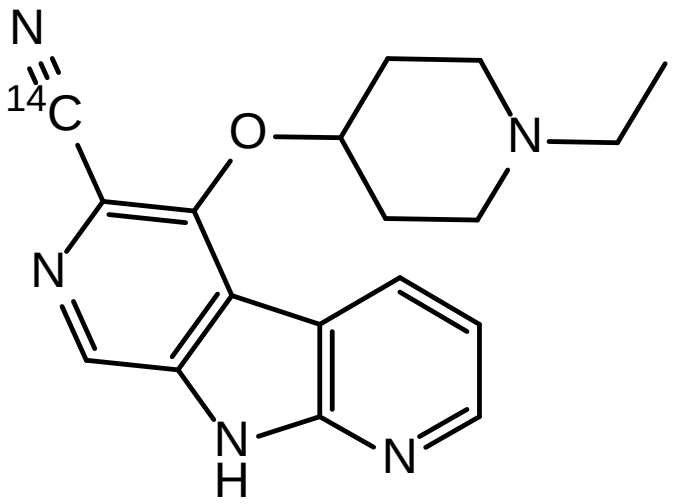

Figure 2

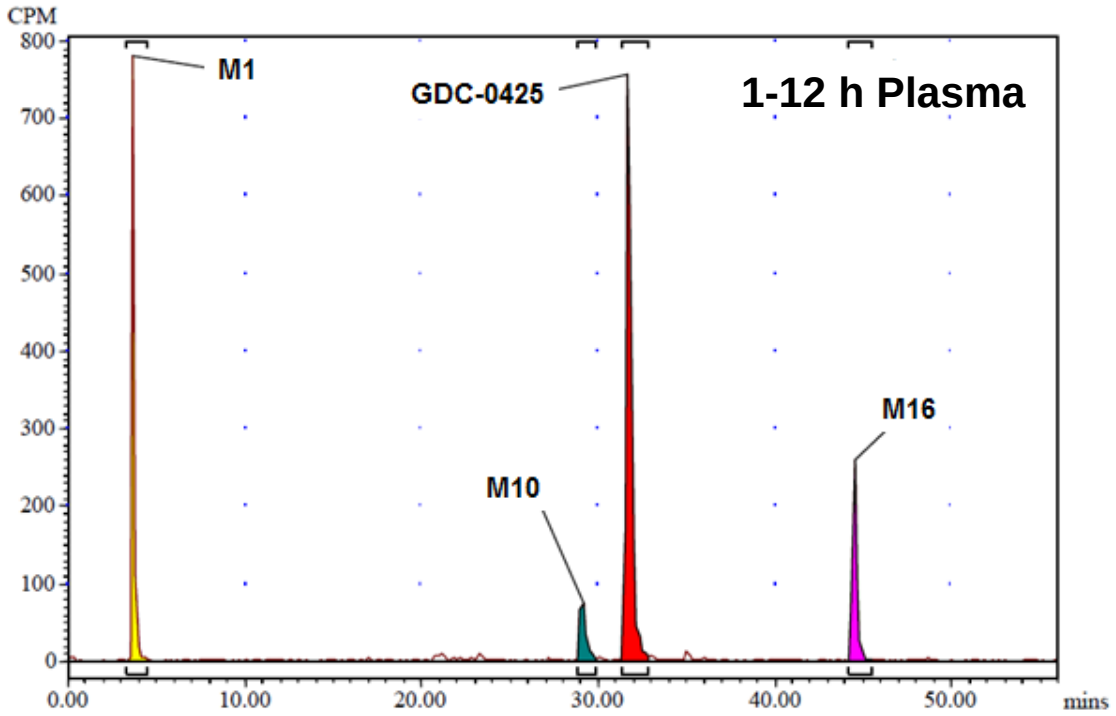

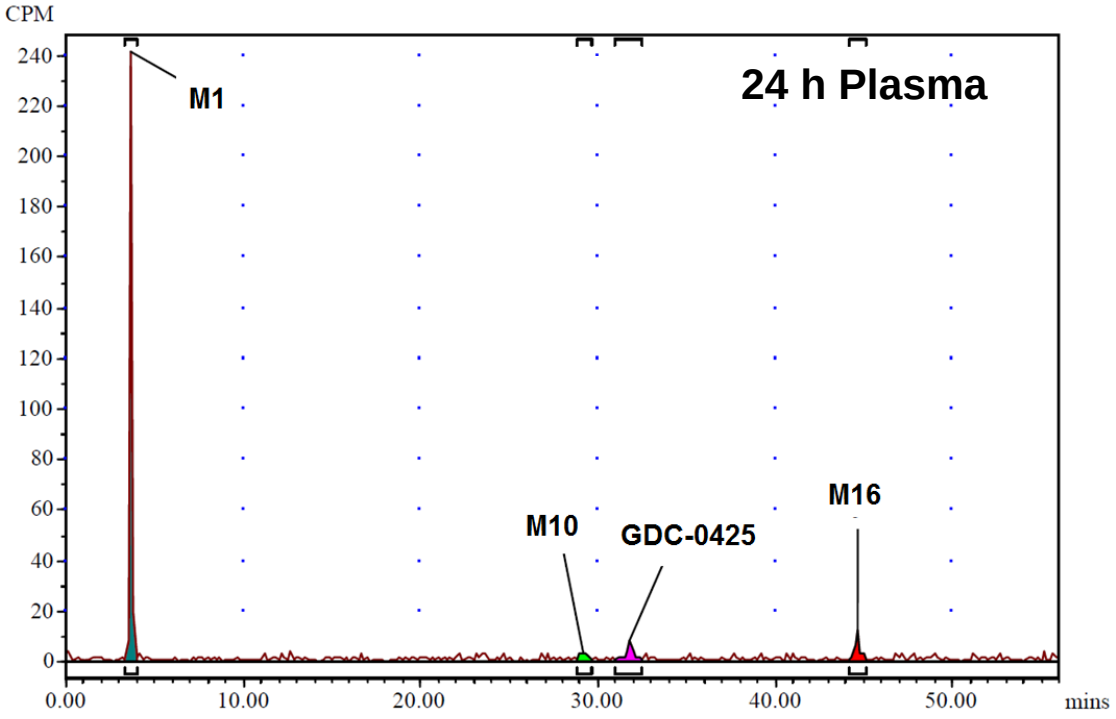

Figure 3

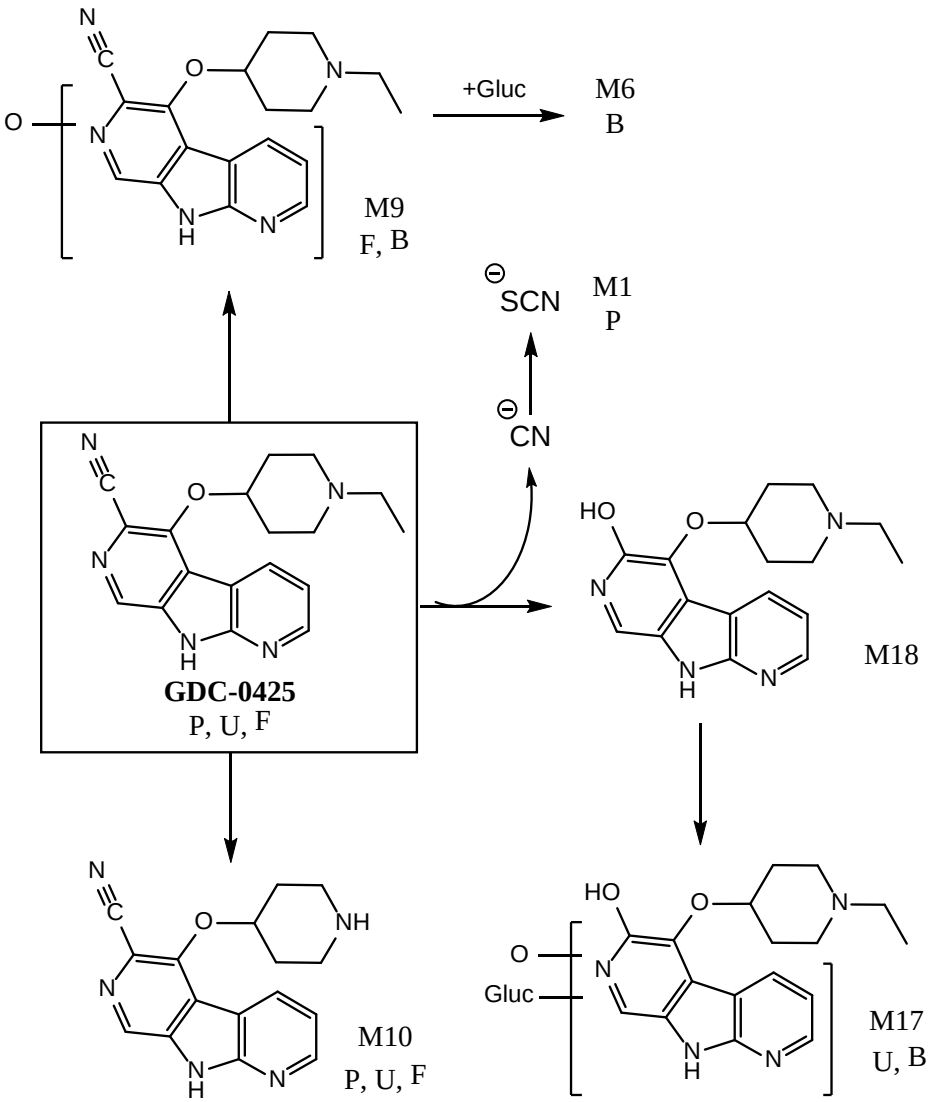

Figure 4

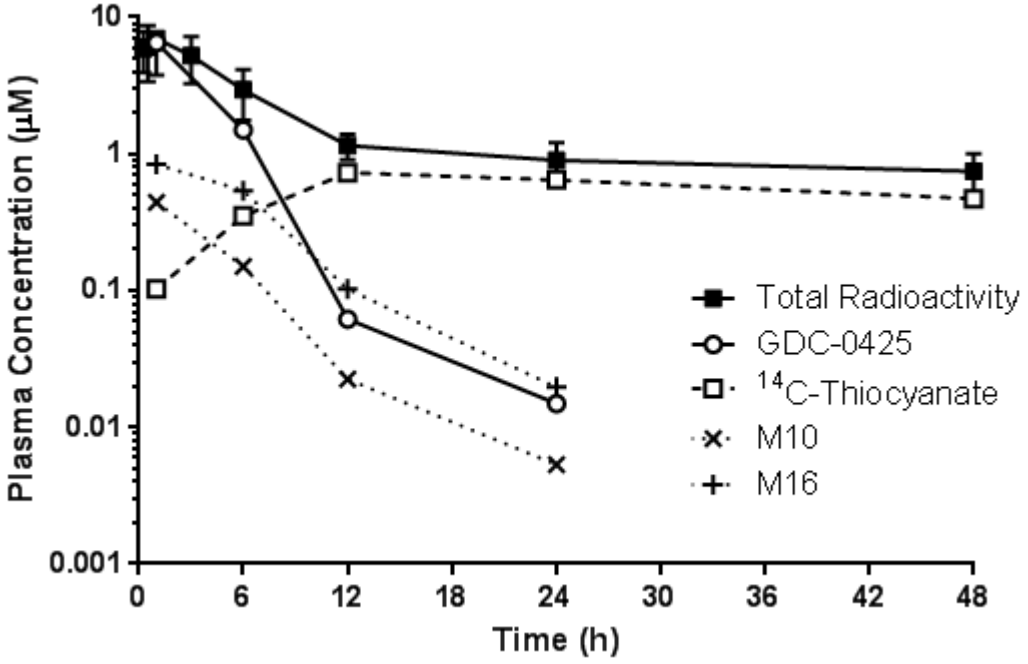

Figure 5

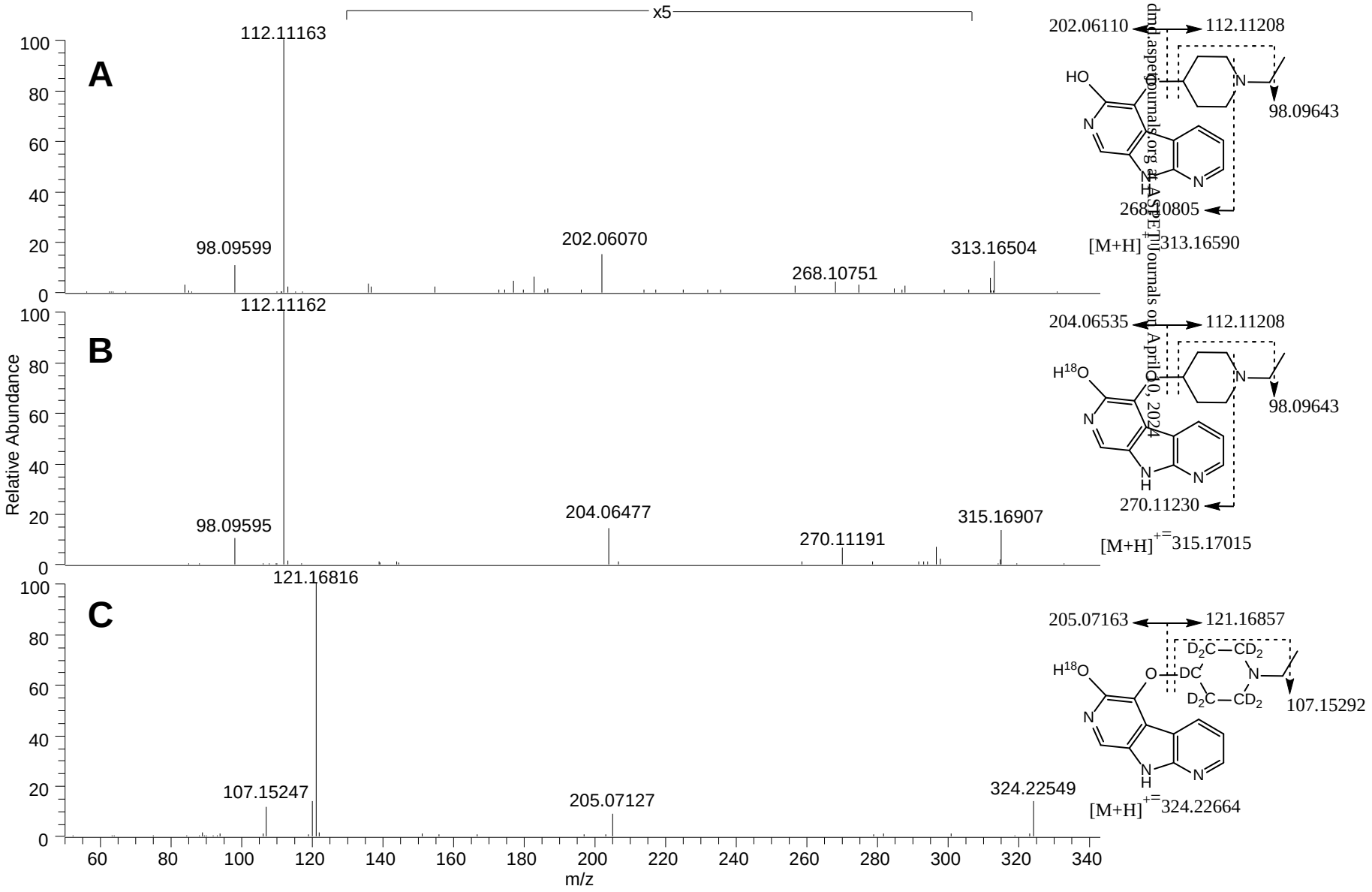

Figure 6

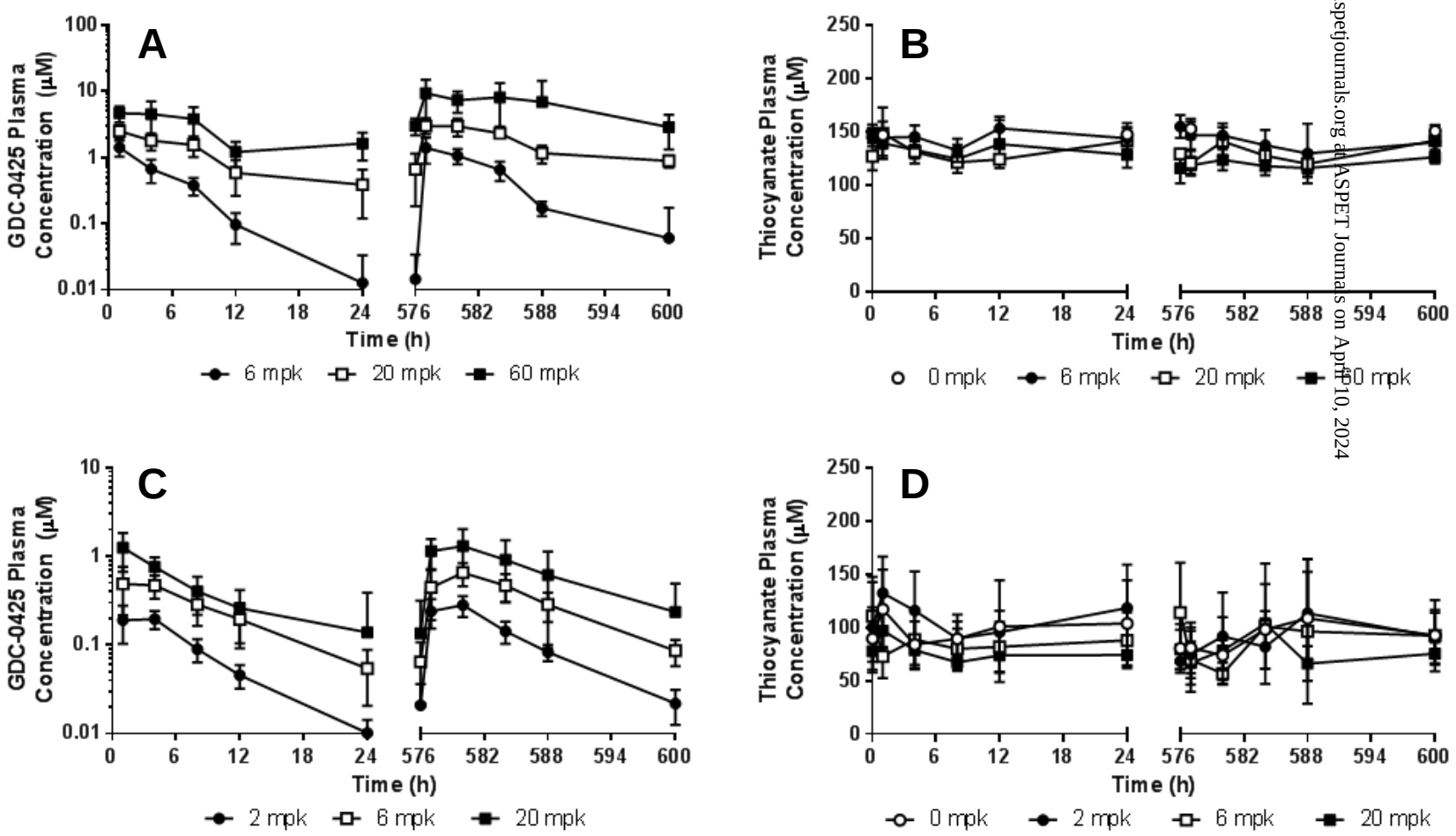

Figure 7

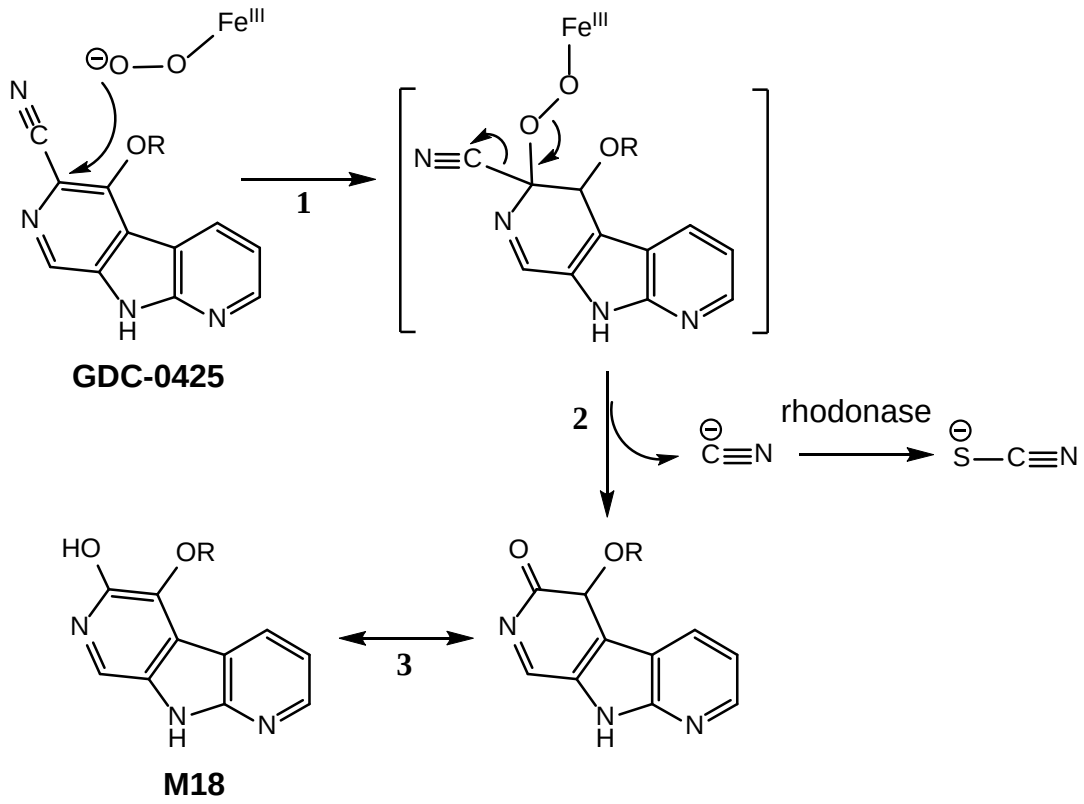

Drug Metabolism and Disposition

Supplemental Material

Novel Mechanism of Decyanation of GDC-0425 by Cytochrome P450

Ryan H Takahashi, Jason S Halladay, Michael Siu, Yuan Chen, Cornelis ECA Hop, S Cyrus Khojasteh, Shuguang Ma

Supplemental Figure 1. Recovery of radioactivity from Sprague-Dawley rats following a single oral administration of [^{14}C]GDC-0425 at 10 mg/kg (200 µCi/kg). Symbols and error bars represent mean and standard deviation from three male and three female rats. (A) Animals were non-surgicalized and (B) animals were bile-duct cannulated.

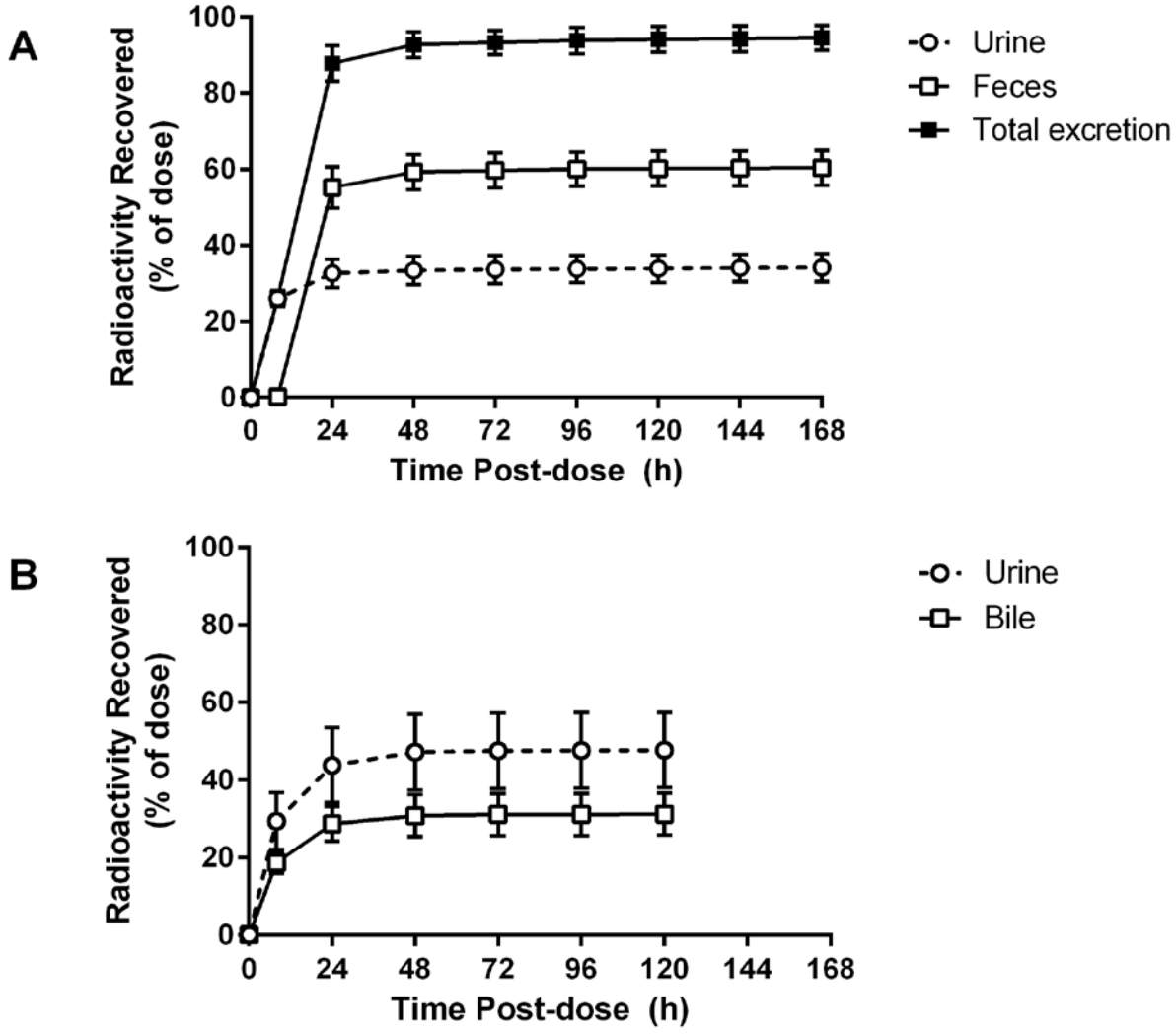

Supplemental Table 1. Plasma concentrations for GDC-0425 and thiocyanate measured in repeated administration studies in Sprague-Dawley rats and cynomolgus monkeys.

Species	Day	GDC-0425 Dose	Sex	GDC-0425			Thiocyanate	
				C_{max} (µM)	T_{max} (h)	$AUC_{0\text{-}24\ h}$ (µM·h)	Mean Conc (µM)	$AUC_{0\text{-}24\ h}$ (µM·h)
Rat	1	0 (vehicle)	Male	-	-	-	154 (8)	3540
			Female	-	-	-	141 (10)	3230
		6	Male	1.37	1.0	6.69	141 (12)	3390
			Female	1.46	1.0	8.37	148 (9)	3580
		20	Male	2.22	1.0	20.6	132 (11)	3160
			Female	2.77	1.0	28.2	133 (20)	3130
		60	Male	5.23	8.0	56.6	137 (15)	3300
			Female	5.66	4.0	62.9	133 (15)	3090
	24	0 (vehicle)	Male	-	-	-	156 (7)	3580
			Female	-	-	-	148 (5)	3400
		6	Male	1.14	1.0	9.77	153 (15)	3590
			Female	1.65	1.0	11.9	132 (13)	3030
		20	Male	3.30	4.0	43.2	132 (12)	3150
			Female	3.10	1.0	37.6	128 (14)	3090
		60	Male	7.44	4.0	111	122 (8)	2900
			Female	11.7	1.0	190	118 (11)	2870
Monkey	1	0 (vehicle)	Male	-	-	-	93.3 (35.3)	2290 (365)
			Female	-	-	-	102 (32.7)	2430 (580)
		2	Male	0.242 (0.05)	4.0	2.08 (0.44)	107 (34.2)	2610 (233)
			Female	0.222 (0.06)	1.0	1.63 (0.31)	110 (30.6)	2500 (506)
		6	Male	0.485 (0.15)	4.0	5.26 (1.89)	80.8 (29.2)	1850 (175)
			Female	0.650 (0.25)	1.0	6.10 (2.41)	93.4 (25.5)	2180 (322)
		20	Male	1.16 (0.44)	1.0	8.37 (3.42)	77.5 (19.4)	1800 (290)
			Female	1.47 (0.57)	1.0	11.0 (3.7)	79.0 (14.4)	1830 (217)
	24	0 (vehicle)	Male	-	-	-	85.7 (24.6)	2260 (234)
			Female	-	-	-	92.6 (28.5)	2310 (516)
		2	Male	0.345 (0.05)	4.0	3.27 (0.36)	87.2 (33.0)	2210 (293)
			Female	0.258 (0.08)	1.0	2.43 (0.58)	86.8 (34.3)	2370 (496)
		6	Male	0.638 (0.24)	4.0	7.28 (2.92)	89.0 (47.8)	2020 (731)
			Female	0.731 (0.17)	4.0	8.49 (1.14)	87.9 (41.8)	2240 (373)
		20	Male	1.08 (0.38)	1.0	12.5 (7.6)	70.7 (16.5)	1660 (212)
			Female	1.76 (0.71)	4.0	21.3 (13.2)	86.1 (39.6)	2040 (325)

For rats, concentration-time profiles were composed from separate animals at individual time points, so error in parameter estimates was not calculated. For monkeys, values are mean (SD) for n=5 animals except t_{max}, which are median. For control animals, plasma samples were for 1 and 24 h post-dose on Day 1 and Day 24